

Research Paper

A Novel Nanocapsule Delivery System to Overcome Intestinal Degradation and Drug Transport Limited Absorption of P-glycoprotein Substrate Drugs

Taher Nassar,¹ Alona Rom,¹ Abraham Nyska,² and Simon Benita^{1,3}

Received February 10, 2008; accepted March 28, 2008; published online June 26, 2008

Purpose. To design a double-coated nanoparticulate delivery system of tacrolimus capable of overcoming the P-glycoprotein pump and CYP3A barriers without affecting their physiological activities.

Materials and Methods. Tacrolimus loaded oil cores were first nanoencapsulated with two polymethacrylate polymers followed by the microencapsulation of these nanocapsules within hydroxypropylmethylcellulose using a spray drying technique. The Trojan effect of these double-coated nanocapsules was evaluated in Caco-2 monolayer by monitoring the tacrolimus uptake and measuring the transport of tacrolimus across the rat jejunum membrane.

Results. The formulation was shown to release nanocapsules rather than dissolved drug under sink conditions. The nanocapsules protected tacrolimus from degradation in the diluted intestinal fluids following 2 h incubation. The Caco-2 and intestinal segment uptake of tacrolimus from the novel delivery system with and without verapamil was significantly higher than the uptake of tacrolimus from the aqueous solution and emulsion. The blank drug delivery system did not inhibit the P-gp pump activity. The nanocapsules internalized rapidly in the enterocytes as confirmed by the histological results.

Conclusion. The overall results suggest that the novel nanodelivery system which does not alter the activity of the P-gp is a potential platform for intestinal transport of sensitive lipophilic molecules that are P-gp substrates.

KEY WORDS: CYP3A; nanocapsules; P-gp; tacrolimus.

INTRODUCTION

The gut wall presents a major challenge for the oral delivery of lipophilic drugs which are poorly soluble in water, rendering difficult their pharmaceutical formulations and seriously limiting their clinical efficacy. During oral absorption, P-glycoprotein (P-gp)-mediated efflux across the apical membrane and cytochrome P4503A (CYP3A)-mediated metabolism in the enterocytes (intestinal absorptive cells) can limit the oral bioavailability of various drugs belonging to different therapeutic classes such as cytotoxic drugs, immunosuppressant agents, HIV protease inhibitors, steroids, antibiotics (1–4). This is in addition to the physical processes (solubility, tissue permeability, formulation factors) that take place in oral absorption (1,2). Oral bioavailability is therefore, a complex process depending on formulation and physiological variables. Thus, inhibition of active efflux is one of the strategies used to improve oral absorption of drugs that are pumped out from the intestinal epithelium into the lumen by efflux transporter systems (5–8). Indeed, first and second generations of P-gp inhibitors succeeded in improving

markedly the oral bioavailability of P-gp substrate drugs in animals. However, their clinical applicability has been limited since they lacked specificity and inhibited two or more ABC transporters. Their administration was also associated with marked adverse effects including failure of the immune system (6). Moreover, since most of the P450/P-gp suppressors exhibit low water solubility their formulation is difficult to achieve (7). With regard to oral drug transport, the development of highly selective P-gp inhibitors can certainly represent an attractive goal to reduce potential toxicity. The latter strategy has been successfully applied for the oral administration of HIV protease inhibitors (8). Ritonavir, at low dose is recognized as both an inhibitor of P-gp and CYP3A across the gut wall, and is used frequently for these effects to increase the bioavailability of co-administered protease inhibitors, thereby reducing the potential for the emergence of resistant viral mutants. Although toxicity is recognized, to date it has not limited the clinical application of this approach, which has been shown to improve the durability of certain anti retroviral treatment regimens (9). Apart from this limited specific commercial success, more effective and safer inhibitors are needed to boost the P-gp inhibition approach. Furthermore, these effective P-gp inhibitors are also considered active compounds in the formulation and thus impose regulatory constraints. Long, fastidious and costly development of novel combination products is needed to allow possible registration and approval by health authorities. Constantinides and Wasan (10) recently reviewed additional

¹ Department of Pharmaceutics, School of Pharmacy, The Hebrew University of Jerusalem, P. O. Box 12065, 91120 Jerusalem, Israel.

² Consultant in Toxicological Pathology, Sackler School of Medicine, Tel Aviv University, Tel Aviv, Israel.

³ To whom correspondence should be addressed. (e-mail: benita@cc.huji.ac.il)

pharmaceutical approaches for enhancing intestinal absorption of P-gp substrate drugs by using excipient inhibitors that exhibit minimal nonspecific pharmacological inhibition activity in the lipid formulations. Until now, only encouraging *in vitro* and animal study results have been published (5,11) although toxic effects resulting from chronic administration of these excipient inhibitors cannot be excluded. Furthermore, attempts were made to improve the oral absorption of P-gp substrates by incorporating the drugs in the inner oil cores of emulsion formulations which exhibited better absorption profiles (12–14). However, the use of these systems was limited due to their poor physical stability and the large volumes needed. Thus, self emulsifying drug delivery systems (SEDDS) which are a promising alternative to orally administered emulsions because of their relatively high physical stability and their ability to be delivered in standard soft gelatin capsules were then proposed (15–17). A multiple dosage study was conducted on humans diagnosed with HIV infection. The study participants were given orally an HIV protease inhibitor either as a SEDDS or as an elixir (17,18). Greater AUC values in addition to higher C_{max} and C_{min} values were reported for patients given the SEDDS as compared to the ones given the elixir. Finally, most of the current delivery solutions including the self-microemulsifying drug delivery systems developed for enhancing the oral absorption of lipophilic P-gp substrate drugs, suffer from limitations owing to the rapid release and partition of the incorporated drug in favor of the gut fluids under sink conditions.

Here, for the first time, we propose a new concept of double coated nanocapsules to improve the uptake of P-gp substrate drugs without affecting the physiological activity of the transporters especially the P-gp pump. Tacrolimus was selected as the model drug in the present study since its oral bioavailability is variable and ranges from 10% to 25% and requires frequent monitoring throughout the entire life of the patients owing to its marked pre-systemic metabolism by CYP3A in the enterocytes and P-gp efflux in addition to liver first pass effect (19–21). The objective of this investigation was to design an advanced novel double coating nanoparticulated delivery system of tacrolimus capable of overcoming these biochemical barriers without affecting their physiological activities in Caco-2 monolayer and isolated rat jejunum segment.

MATERIALS AND METHODS

Materials

Poly(ethyl acrylate, methyl methacrylate, trimethylammonioethyl methacrylate chloride) 1:2:0.1 (Eudragit[®] RS) and poly(methacrylic acid, ethyl acrylate) 1:1 (Eudragit[®] L100-55) were purchased from Rohm (Darmstadt, GmbH, Germany). Hydroxypropylmethylcellulose (Methocel E4M Premium) was obtained from Dow Chemical Company (Midland, MI, USA), Argan Oil was purchased from Alban-Muller (Vincenny, France), oleoyl polyoxylglycerides (Labrafil M 1944 CS) was kindly donated by Gattefosse (St. Priest, France), tacrolimus (as monohydrate) was purchased from Concord Biotech Limited (Ahmedabad, India). Other chemicals and solvents were of analytical reagent grade and double-distilled water was used throughout the study. The commercial

tacrolimus capsule product, Prograf[®] manufactured by Fujisawa Ltd. UK was purchased from a retail pharmacy (Batch number 5C5129B).

Preparation of the Nanocapsules

The primary nanocapsules were first prepared by dissolving in a solution of 95 ml of acetone and 5 ml of absolute ethanol, the following compounds: 500 mg of argan oil, 100 mg of oleoyl polyoxylglycerides, 250 mg of Eudragit RS, 750 mg of Eudragit L and 20 mg of tacrolimus when needed. Then, purified water was added to the organic phase at a constant rate of 20 ml/min using stepdos 03RC pump (KNF Folds, Sursee, Switzerland). An o/w emulsion was formed as evidenced by the rapid formation of opalescence in the dispersion medium. In some of the formulations, samples were withdrawn at 10, 20, 30 s and 1, 2, 3, 4 min and examined by optical microscopy using an Olympus BX 40 light microscope (Olympus, Tokyo, Japan) at X 200 magnification and a Sony DXC-3900 video camera (Sony Corporation Tokyo, Japan). Nanocapsule size measurements for each sample were carried out utilizing the ALV sizer as detailed below. Preliminary formulations were prepared and evaluated by varying the process parameters including the blend ratio of the Eudragits. An optimal formulation with a specific Eudragit blend ratio was selected for further studies: Eudragit L: Eudragit RS 750:250 (3:1). A formulation consisting of the identical oil core phase (same concentrations) without the wall coating polymers was also prepared and defined herewith as the “emulsion”.

Microsphere Preparation

The microspheres were formed by microencapsulating the tacrolimus loaded nanocapsules using the spray drying technique. Once the nanocapsules were formed, 200 ml of 0.5% hydroxypropylmethylcellulose (HPMC) solution was added to the dispersed solution, prior to the spray drying procedure. The suspension was spray-dried with a Buchi mini spray-drier B-190 apparatus (Flawil, Switzerland) under the following conditions: inlet temperature 180°C; outlet temperature 113°C; aspiration 50%; feeding rate of the suspension was 2.5 ml/min. The powder was then collected in the cyclone separator and the outlet yield was calculated. The formulations with the Eudragit blend ratios of L:RS of 3:1 were denominated Nof-29. All the batch formulations were triplicated.

Physicochemical Characterization of Nanocapsules and Subsequent Microspheres

Drug Content

The total amount of the drug in the powder was analyzed by dissolving the sample in 5 ml of PBS. After the polymer was dissolved, 1 ml of acetonitrile (ACN) was added and the mixture was stirred (100 rpm) over 1 h. Thereafter, 3 ml of ethyl acetate were added and the mixture was stirred vigorously and centrifuged at 4,000 rpm for 5 min.

The extraction of tacrolimus by ethyl acetate was repeated three times to ensure total removal of the drug from the mixture. The different ethyl acetate layers (upper

layer) were transferred to a clean tube and evaporated under air to dryness. The combined residues were dissolved in 1 ml of ACN, and 50 μ l were injected into HPLC under the following conditions: Mobile phase—acetonitrile 100%, flow rate—0.5 ml/min, wavelength—213 nm, Column—LiChrospher® 100 RP-18 (5 μ m), 4/120 mm. A calibration curve constructed from tacrolimus concentrations ranging between 5 to 250 μ g/ml yielded a linear correlation ($r^2=0.999$).

The detection limit of tacrolimus was found to be 3.9 μ g/ml. The tacrolimus incorporation yield was calculated by the following equation:

$$\text{Drug yield(\%)} = \frac{\text{Amount of the drug detected}}{\text{Amount of the drug incorporated}} \times 100 \quad (1)$$

Determination of Particle Size of the Primary Nanocapsules and Secondary Microspheres

Nanocapsule size measurements were carried out utilizing an ALV non-invasive back scattering high performance particle sizer (ALV-NIBS HPPS; Langen, Germany) at 25°C and using water as the solvent. A laser beam at 632 nm wavelength was used. The sensitivity range was 0.5 nm–5 μ m. Spray dried microspheres were qualitatively evaluated by scanning electron microscopy.

Optical, Transmission (TEM) and Scanning Electronic Microscopy (SEM) Studies

Morphological evaluation of nanocapsules and spray dried microspheres was carried out using optical and scanning electron microscopy (model: Quanta 200, FEI, Germany). The samples were fixed on a SEM-stub using double-sided adhesive tape and then made electrically conductive following standard coating by gold sputtering (Pilon E5100) procedure under vacuum. In addition, morphological evaluation of nanocapsules was performed using TEM analysis. The sample was placed on a collodion-coated, carbon-stabilized, copper grid for 1 min and stained with 1% phosphotungstic acid (PTA). The samples were dried and examined by TEM (Phillips CM-12; Philips, Eindhoven, The Netherlands).

In-vitro Stability of Tacrolimus in Rat Intestinal Juice (pH 6.5)

The following solutions were added sequentially to a test tube: 300 μ l of freshly thawed intestinal juice, 60 μ l of 0.6 M phosphate buffer, pH 6.5 (the pH of the mixture of intestinal juice) and 25 μ g/ml of tacrolimus in various formulations (up to 1.5 ml). The mixtures were stirred and incubated at 37°C over time. At given time intervals of 5, 10, 20, 30, 45, 60, 90 and 120 min, the samples were withdrawn from the incubation, mixed with 150 μ l of 0.5 M hydrochloric acid and 2 ml of ethyl acetate. The resulting mixtures were stirred vigorously and centrifuged at 4,000 rpm (equivalent to 3,000 \times g) over 10 min. The extraction of tacrolimus by ethyl acetate was repeated three times to ensure total removal of the drug from the mixtures as already described above. The combined residues were dissolved in 1 ml of acetonitrile, and 50 μ l were injected in the HPLC under the conditions described above.

Caco-2 Uptake Study

Caco-2 monolayers (passage 73) were grown in Dulbecco's modified Eagle's medium supplemented with 10% fetal bovine serum, 1% L-glutamine, 1% nonessential amino acids, and 5% antibiotic-antimycotic solution at 37°C in humidified air, 5% CO₂ atmosphere. The culture medium was initially replaced after 72 h and every 48 h thereafter. The uptake studies were conducted with monolayers between 8 to 10 days in culture. All diffusion experiments were performed over 1 h at 37°C. Prior to the experiments, the culture medium was replaced with transport medium and cell monolayers were subsequently equilibrated for 30 min at 37°C before the uptake study. Transport medium was Hanks buffer composed of 136.89 mM NaCl, 5.36 mM KCl, 0.34 mM Na₂HPO₄, 0.44 mM KH₂PO₄, 0.41 mM MgSO₄·7H₂O, 19.45 mM glucose, 1.26 mM CaCl₂, 0.49 mM MgCl₂·6H₂O, 4.17 mM NaHCO₃, 10 mM HEPES, and the pH was adjusted to 7.4. At the end of the experiments, the transport medium (1.5 ml) was withdrawn to a clean tube to determine the tacrolimus levels in HPLC. The cell monolayer was washed 3 times with 1 ml Hanks solution and then combined with the transport medium. As for the cell monolayer in the wells, 1.5 ml of 1% SDS was administered into each well to undergo lysis of the cell monolayer. The lysate was collected in a clean tube and tacrolimus was determined by HPLC as described above. When verapamil, a well-known CYP3A substrate and P-gp inhibitor (22) was used, the concentration in the medium was 150 μ g/ml and the Caco-2 cells were pre-incubated with the verapamil solution 30 min prior to the transport experiments. Two separate and independent sets of cell culture experiments were carried out with similar tacrolimus formulations but different combinations to verify either the reproducibility and efficiency of Nof-29 or the effect of the blank Nof-29 formulation on the P-gp pump activity. The experiments were quadruplicated. The P-gp expression of the Caco-2 cells was validated using monoclonal antibody C219 directed against the P-gp according to the technique described by Schrickx and Fink-Gremmels (23). Caco-2 cells were fixed in paraformaldehyde (3.6% in PBS) for 15 min and treated with 0.1 M glycine for 5 min. After washing three times they were permeabilized with Triton X-100 (0.1%, w/v) for 15 min and washed again three times. For labeling with antibodies, the sandwich technique was used. Preparations were incubated for 1 h with the primary antibody (1:40), i.e., the specific anti P-gp (C219) purchased from Alexis Biochemicals (San Diego, USA). As a secondary antibody, Rhodamine-labeled anti IgG (1:50) was applied for 1 h. After washing again (three times), the cells were mounted in a mixture of 7 ml of glycerol 100%, 3 ml of 0.1 Tris-HCl, pH 9.5, and 0.5 g of *n*-propyl gallate. Immunohistochemistry images were taken by Olympus 1X71 microscope using Olympus \times 40 lens magnification.

The apparent permeability (P_{app} , cm/s) was calculated according to the following equation described by Schrickx and Fink-Gremmels (23):

$$P_{app} = \frac{Q}{A \times C_o \times t} \quad (2)$$

Where Q is the total amount of permeated drug throughout the incubation time period (μ g t⁻¹), A is the

diffusion area (cm^2), C_0 is the initial concentration ($\mu\text{g/ml}$) and t is the incubation time in seconds.

Transport of Tacrolimus Across the Intestinal Membrane Via an *In Vitro* Diffusion Chamber

All the animal studies in this research were carried out in accordance with the rules and guidelines concerning the care and use of laboratory animals MD 104.01-3 and were approved by the local ethical committee of laboratory animal care at The Hebrew University of Jerusalem.

The tacrolimus across the rat intestinal membrane was studied with the Ussing diffusion chamber (24). Sprague Dawley rats, weighing 280–350 g, were fasted overnight and then anesthetized with sodium pentobarbital (30 mg/kg). The intestine jejunum was exposed through a midline abdominal incision, removed, and washed in ice-cold saline. Intestinal segments were isolated and immersed in ice-cold KRBS. Segments were cut open, the intestinal sheets were mounted onto the pins of the cells, and the half-cells were clamped together. Drug solutions and formulation (7 ml) were added to the donor site with an initial concentration of 25 $\mu\text{g/ml}$, whereas the same volume of drug-free buffer was added to the opposite site. The temperature of cells was maintained at 37°C, and both fluids were circulated by gas lift with 95% O_2 /5% CO_2 . When verapamil was used, the concentration in the medium was 150 $\mu\text{g/ml}$ and the intestinal segments were pre-incubated with the verapamil solution 30 min prior to the permeation experiments. During the transport studies, aliquots were taken from the serosal side and the permeated tacrolimus was assayed by HPLC as described above. It should be mentioned that prior to the permeability studies, the serosa was removed from the jejunum segments. The experiments were quadruplicated.

The apparent permeability (P_{app} , cm/s) was calculated according to the following equation (25)

$$P_{\text{app}} = \frac{V}{A \times C_0} \cdot \left(\frac{dC}{dt} \right) \quad (3)$$

Where A is the diffusion area (cm^2), V is the medium volume in the chamber (ml) and C_0 is the initial concentration ($\mu\text{g/ml}$), and (dC/dt) is the concentration change over time (permeation rate, $\mu\text{g ml}^{-1} \text{s}^{-1}$).

Fluorescent Histological Studies

Male Sprague Dawley rats ($N=9$) were used in this study. The animals were divided into three groups. Following overnight fasting conditions, the animals were dosed by oral gavage, of Nile red, a lipid fluorescent marker incorporated in the Control (saline), argan/labrafil oil phase and Nof-29 (1 mg/ml oil phase). Thirty minutes after dose administration the animals were sacrificed and a 10 cm segment of the jejunum was dissected and fixed in 4% neutrally buffered formalin for further histology analysis. The samples were prepared using cryostat sectioning. Images were taken using a Nikon TE-2000S (Nikon, Melville, NY, USA) inverted fluorescence microscope with a plan Apo 60 \times objective lens (Nikon) and a Hammamatsu CCD ORCAII camera (Hammamatsu, Tucson, AZ, USA) in 488 nm excitation

wavelength and 515 nm wavelength of emission. Images were all deconvolved with SimplePCI software (Improvision, Coventry, UK) and processed using Photoshop 7 software.

Statistical Tests

Differences were analyzed by one-way analysis of variance (ANOVA) for the Caco-2 monolayer and intestinal transport studies. The tests were applied to the curves and calculated parameters. Analysis was determined with the Tukey–Kramer multiple comparisons test calculated by InStat software (version 3.01). The level of significance was corrected using a post test analysis. Statistical significance was set with one asterisk for $p < 0.05$ and with triple asterisk for $p < 0.001$ while values are presented as mean \pm SD.

RESULTS AND DISCUSSION

Recently, investigators have designed lipid nanospheres embedded in microparticles for oral enhanced bioavailability of clozapine which is not a P-gp substrate but undergoes liver first pass-effect (26). Other researchers attempted to improve the oral bioavailability of P-gp drug substrates by providing a proof of principle for a solid tablet dosage form based on thiolated chitosan using rhodamine-123 as the representative of the P-gp substrates. Thiolated chitosan has been reported to modulate drug absorption by inhibition of the intestine P-gp and was the major excipient in the formulation of compressed tablets of 10 mg containing rhodamine-123. The tiny tablets were enterocoated with Eudragit L prior to oral administration to rats. The tablets significantly enhanced the oral bioavailability of the rhodamine-123 owing to the P-gp inhibitory effect of the thiolated chitosan (27). In contrast, we succeeded in designing a novel delivery system which releases nanocapsules containing tacrolimus from swellable microspheres able to cross the intestinal epithelial membrane without modulating the normal activity of the P-gp pump simply by hiding the P-gp substrate within the oil core of the nanocapsules and avoiding any molecular contact between the pump and the drug. The choice of the excipients comprised in the organic phase depends on their ability to solubilize the active ingredient. Argan oil, a long chain triglyceride with labrafil M1944CS exhibited good tacrolimus solubility properties; and therefore this combination was selected for the actual study.

Nanocapsule Loaded Microsphere Preparation and Characterization

The primary nanocapsules (ranging in size from 400–500 nm) were first prepared by slowly adding 80 ml of bi-distilled water to the 100 ml of organic phase within 4 min. The pictures a, b, c in Fig. 1 represent the optical observations of the nanocapsule dispersion following addition of 6.6, 10 and 60 ml of water respectively. Pictures d, e, f represent the droplet size distribution of samples a, b, c respectively. The peaks reflect the size of the droplet populations within the samples at a given time interval. The Nile red fluorescent probe was incorporated in the oil phase to allow a better optical observation as observed in picture c of Fig. 1. It was not possible to nanoencapsulate all the oil cores present in the

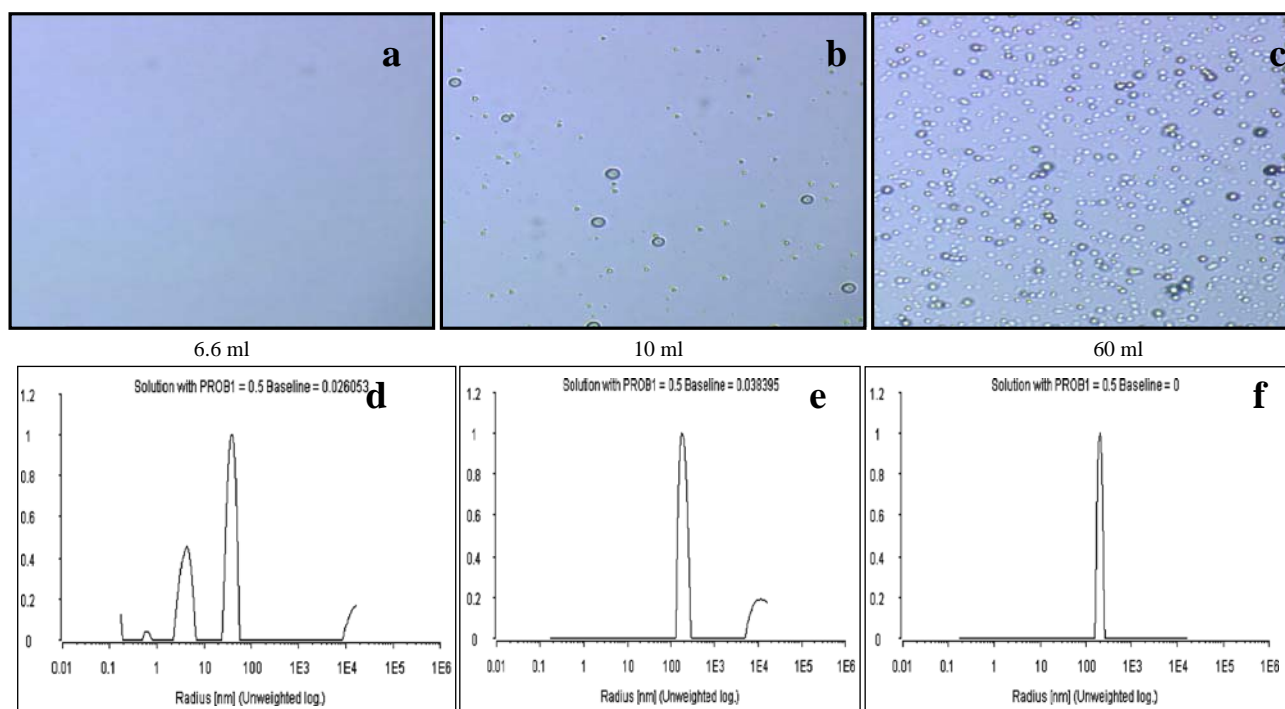


Fig. 1. Optical photomicrographs and particle size distribution of nanocapsules following progressive addition of water to 100 ml acetone/ethanol (19:1) solution comprising argan oil, oleoyl polyoxyglycerides and a blend of Eudragit L:RS, 3:1. Nile red (1 mg/ml oil phase) was used as a marker. The pictures **a**, **b**, **c** represent the optical observations of the nanocapsule dispersion following addition of 6.6, 10 and 60 ml water respectively. Pictures **d**, **e**, **f** represent the droplet size distribution of samples **a**, **b**, **c** respectively. The peaks reflect the size of the droplet populations within the samples at a given time interval. The Nile red was incorporated in the oil phase to allow a better optical observation.

formulation using the well-established solvent displacement method where the acetone organic phase is added to the aqueous phase (28). Some free oil droplets were detected at the surface of the colloidal dispersion irrespective of the initial oil/acetone/ethanol ratio. Surprisingly, when the water phase was slowly added to the organic phase; the water first dissolved in the acetone/ethanol/oil phase or formed probably a w/o microemulsion as a result of the presence of the oleoyl polyoxyglycerides lipophilic surfactant which exhibits an HLB value of 4. In addition, when the samples with different amounts of added water were analyzed for particle size distribution, an interesting phenomenon was observed as depicted in Fig. 1d–f. At low amounts of water (6.6 ml), different tiny particle size populations well below 100 nm were observed (Fig. 1d). This is probably the stage where small unstable water droplets, undetected by optical microscopy examinations, coalesced. On further addition of water (10 ml), an increase in particle size up to 2,000 nm was noted with lesser variability (Fig. 1e), until the system stabilized when the amount of water reached 60 ml. Then, the particle size distribution exhibited a narrow range as reflected by the sharp peak with an average diameter of 400 nm (Fig. 1f). The progressive increase in water concentration in the acetone lipophilic phase apparently led to an emulsion phase inversion process from w/o to o/w mediated by the coalescence of the water droplets as normally occurring in the process of o/w emulsion preparation when the external aqueous phase is progressively added to the oil phase (phase inversion approach) (29). At this stage, as already reported (28,30), the rapid diffusion of the acetone/ethanol from the inner oil phase

towards the external aqueous phase occurred resulting in the deposition of the hydrophobic polymers at the o/w interface and formation of nanocapsules which consisted of an oil core coated by the Eudragit polymer blend. Upon further addition of water up to 60 ml, the nanocapsule population growing simultaneously as depicted in Fig. 1c. No additional changes were observed up to the final ratio of acetone solution to water of 100:80 v/v. It should be stressed that the nanocapsule process formation was carried out at a pH of 4–4.5 below the Eudragit L solubility pH level.

Discrete individual nanocapsules could be detected by TEM observations following the addition of 200 ml of water containing 0.5% HPMC confirming the previous optical findings (Fig. 2a). The formation of the polymeric envelopes around the oil droplets was evidenced by TEM and SEM observations. It should be emphasized that the thickness of these polymeric envelopes was much smaller than 10 nm as qualitatively estimated from the TEM observations (data not shown). The total dispersion was then subjected to spray drying to remove all the aqueous and volatile dipolar solvents. The expected enhanced availability and protection of the drug in the gastro-intestinal environment was achieved by first nanoencapsulating the drug loaded oil cores with a combination of two polymethacrylate polymers, one of them pH sensitive (Eudragit[®] L, soluble above pH 5.5 whereas Eudragit RS is insoluble irrespective of the pH) followed by the microencapsulation of these nanocapsules within a bioadhesive gel forming polymer, HPMC from an aqueous solution. The final product was a powder comprised of microspheres with a mean diameter of $6 \pm 4 \mu\text{m}$ as estimated

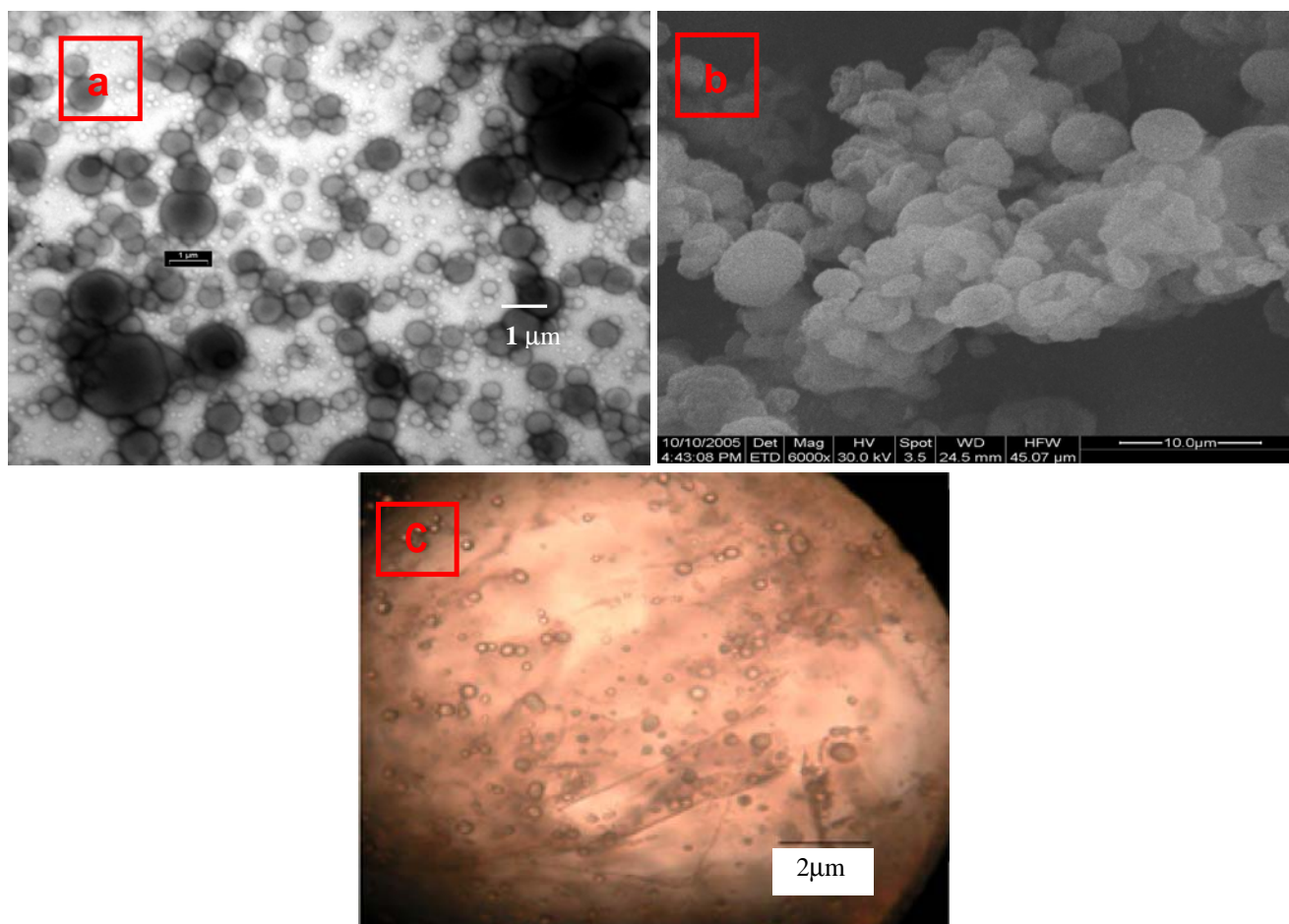


Fig. 2. **a** TEM micrograph of the nanocapsule formulation (polymeric envelope consisting of the Eudragit blend L: RS, 3:1) diluted with the hydroxypropylmethylcellulose solution, **b** SEM micrograph of the resulting microspheres (formulation Nof-29, the nanocapsules are embedded in the spherical matrices and cannot be detected by SEM) following spray drying (**c**) photomicrograph of a typical microsphere from the same batch (Nof-29) following 2 min incubation in phosphate buffer pH4.8.

from Fig. 2b. It can be noted from the optical observations that these microspheres indeed comprised nanocapsules (Fig. 2c). Furthermore, the optical observations depicted in Fig. 3, showing the behavior of the microspheres at different pH solution, suggest that the microsphere matrices are comprised not only of HPMC but also of the Eudragit RS and L that did not participate in the formation of the nanocapsule coatings. At pH smaller than 5 (Fig. 3a) no rapid swelling of the matrices occurred whereas at pH 7.4 Eudragit L dissolved rapidly and contributed to the rapid swelling and partial dissolution of the spherical micromatrices within less than 5 min leading to the leakage/release of nanocapsules (Fig. 3b,c). It was not possible to distinguish any regular morphological structure following a 3 h incubation of the spray dried microspheres in the release medium pH 7.4 over 3 h using SEM examination. Apparently, the secondary HPMC coating and most of the Eudragit blend excess consisting of Eudragit L dissolved and no defined structures could be identified. The nanocapsules are therefore expected to be released from such a delivery system in the intestinal environment where the pH is above 6.5.

The final tacrolimus content was in the three Nof-29 batches 7.3, 5.2 and 7.0 mg/g while the theoretical content was 7.6 mg/g. The average content was 6.5 ± 1.13 mg/g showing a range deviation of 17% and a mean entrapment yield of 85%.

Similar behavior was noted with other formulations. The observed deviation range can be considered reasonable taking into consideration that laboratory formulation process parameters can be better controlled and markedly improved during the scaling up and validation phases. Further improvement and optimization of the formulation is needed.

The follow up of the chemical stability by HPLC of the spray dried powdered formulations showed that tacrolimus is stable at least over three months storage at 37°C. It can clearly be noted from the data depicted in Fig. 4 that tacrolimus incubated only with PBS at pH 6.5 [control (-)] remained intact and no degradation could be observed over 120 min incubation. However, upon addition of rat intestinal juice to PBS (1:5, v/v) [control (+)], a rapid degradation occurred reducing the initial concentration (25 μg/ml) by at least 50%. It is interesting to note that the formulation of tacrolimus in an emulsion or the commercial product, Prograf® cannot protect tacrolimus from the enzymatic degradation in the intestinal juice whereas the microencapsulation of the tacrolimus loaded nanocapsules (Nof-29) elicited a marked enzymatic protection since only 20% of the initial tacrolimus concentration was decomposed. Apparently, tacrolimus was slowly released from the double-coated nanoparticulate delivery system and only the portion of drug released was subject to enzymatic degradation as expected.

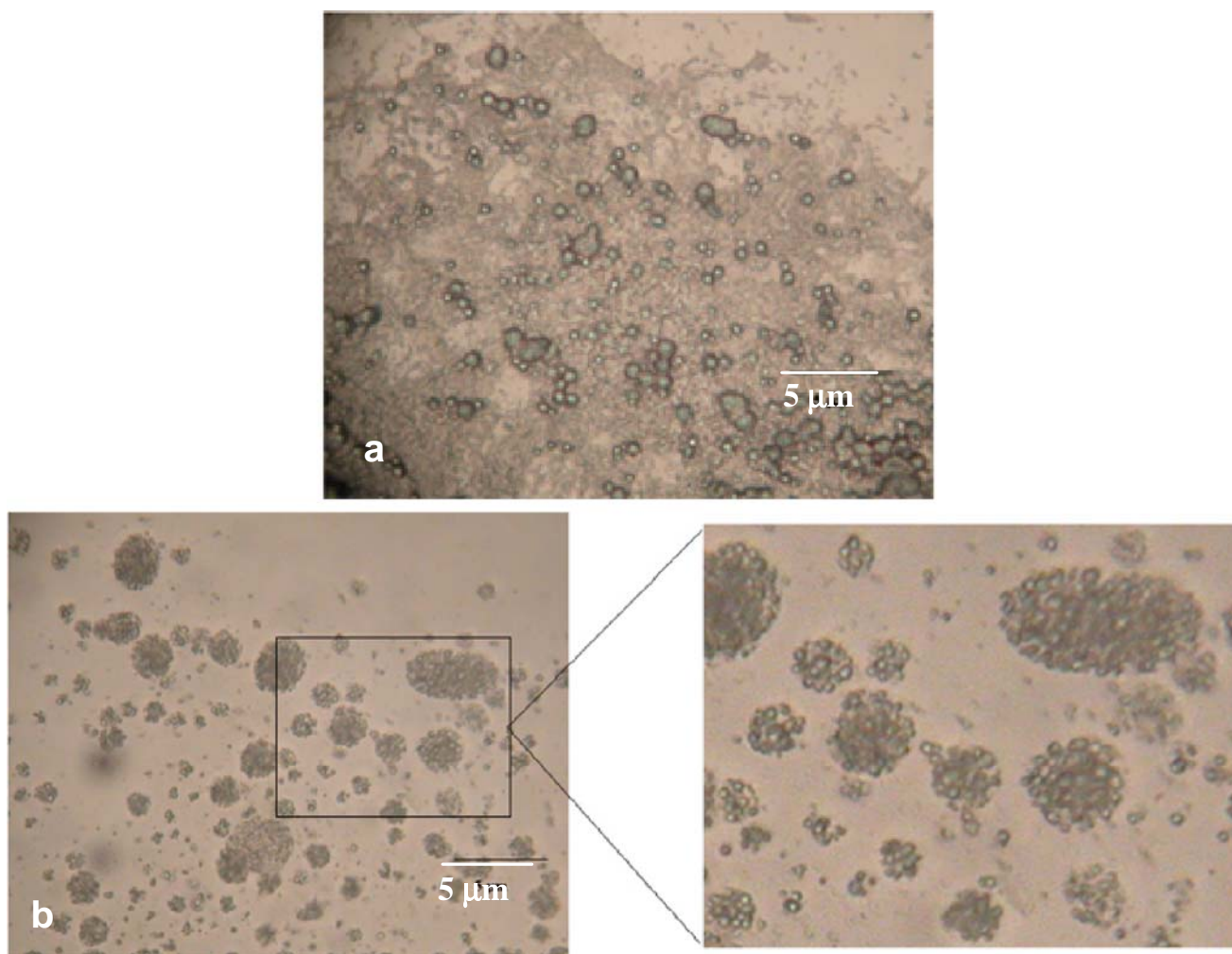


Fig. 3. Photomicrograph of **a** embedded nanocapsules prepared with Eudragit L:RS (3:1) nanocapsule coating and HPMC matrix (Nof-29) following 5 min incubation with phosphate buffer (pH 4.8), **b** embedded nanocapsules (Nof-29) following 3 min incubation with phosphate buffer (pH 7.4).

These results clearly demonstrated that the novel dosage form is able to protect significantly the sensitive drug from the enzymes present in the intestinal juice.

Tacrolimus Uptake in Caco-2 Monolayer

Monolayers of differentiated Caco-2 cells show morphological and biochemical similarity to normal intestinal enterocytes, and they develop effective tight junctions (23,31). Thus, Caco-2 cell monolayer is considered an established model to investigate the mechanisms involved in oral absorption including the effect of the P-gp pump (31,32). The P-gp expression of the actual Caco-2 monolayer was evidenced (data not shown) using the validated monoclonal antibody C219 technique (23). It can clearly be seen as compared to the control that the Caco-2 cells elicited marked fluorescence demonstrating the affinity binding of the secondary antibody to the Caco-2 cell membranes as a result of the recognition of the P-gp by the C219 antibody.

Tacrolimus residual concentration in the wells with no Caco-2 cells remained constant and diminished moderately in the presence of Caco-2 cells from the apical side when dissolved in Hanks buffer or in the argan oil/oleoyl polyoxyglycerides

phase (Fig. 5a). The tacrolimus concentration decreased significantly in the presence of verapamil, a well-known P-gp inhibitor and CYP3A substrate (22) showing a marked uptake by the Caco-2 cell monolayer. It should be emphasized that the

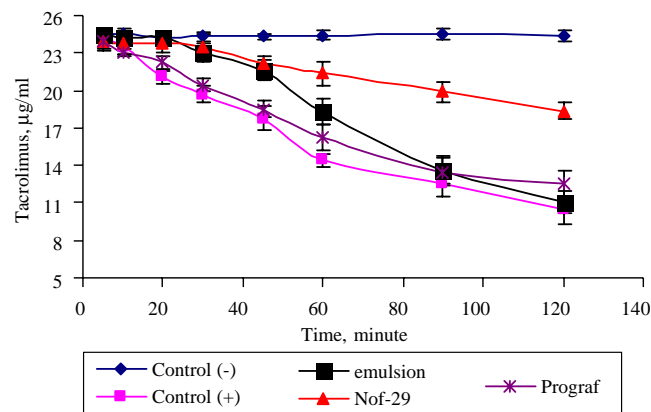


Fig. 4. Tacrolimus stability following incubation of various formulations in rat intestinal juice diluted with PBS (1:5 v/v; pH 6.5) as a function of time.

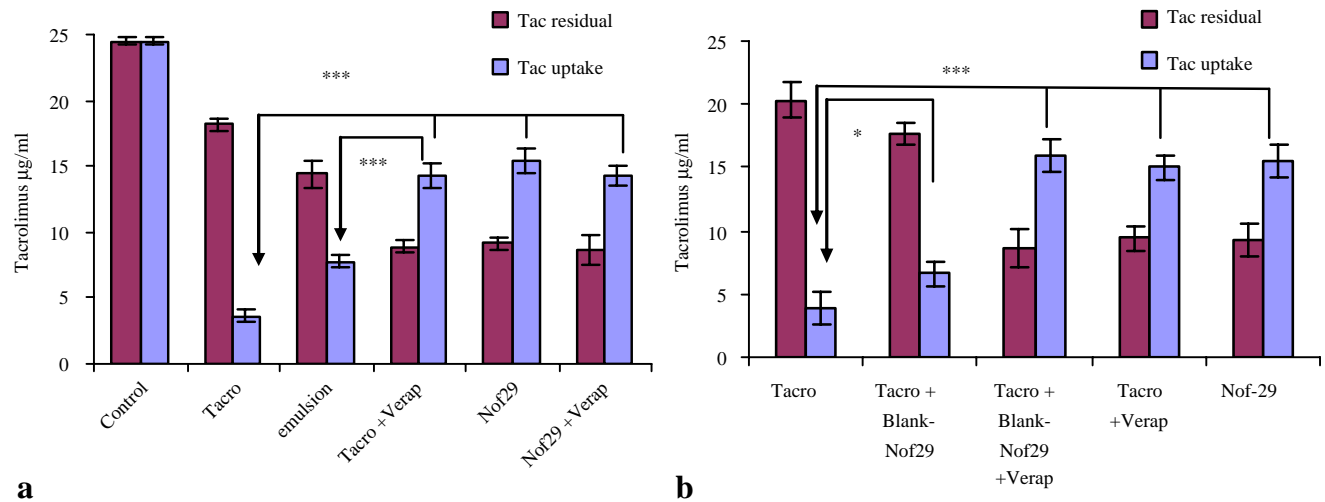


Fig. 5. a Tacrolimus residue in Hanks buffer (pH 7.4) following 60 min incubation in Caco-2 cell monolayer and respective tacrolimus uptake following washing and cell lysis (SDS 1%) of various formulations containing 25 µg/ml tacrolimus. **b** Influence of the blank novel DDS on tacrolimus residue in Hanks buffer (pH 7.4) following 60 min incubation in Caco-2 cell monolayer and respective tacrolimus uptake following washing and cell lysis (SDS 1%) of various formulations containing 25 µg/ml tacrolimus. The concentration of verapamil when appropriate was 150 µg/ml. $N=4$ in all the experiments.

concentration of tacrolimus from the novel DDS (Nof-29) was also low and adding verapamil to the Nof-29 formulation did not further decrease the concentration of tacrolimus (Fig. 5a). This was also confirmed by the data presented in Fig. 5b showing the respective tacrolimus uptake by the Caco-2 cell monolayer. The highest drug uptake was achieved by the tacrolimus solution combined with verapamil and Nof-29 either alone or in combination with verapamil, suggesting that verapamil had no effect on tacrolimus absorption elicited by Nof-29 formulation. Statistical analysis of the apparent permeability (P_{app}) values calculated from Eq. 2, clearly indicated that there was no significant difference between the tacrolimus and verapamil formulation, Nof-29 formulation with and without verapamil (respective values of $8.07 \pm 0.50 \times 10^{-6}$, $8.71 \pm 0.53 \times 10^{-6}$ and $8.08 \pm 0.46 \times 10^{-6}$ cm/s). However, these P_{app} values were significantly higher than the values yielded by the reconstituted emulsion ($4.4 \pm 0.24 \times 10^{-6}$ cm/s) and the tacrolimus aqueous solution ($2.05 \pm 0.26 \times 10^{-6}$ cm/s). Again, under the given experimental conditions, the emulsion could not retain the dissolved tacrolimus in the oil droplets and part of it partitioned in favor of the medium from where it could penetrate the Caco-2 cells and be effluxed as the normal tacrolimus dissolved in the aqueous solution. Furthermore, it can be noted from a second set of experiments, the data of which are depicted in Fig. 6b, that the blank Nof-29 formulation in presence of tacrolimus solution, moderately enhanced the drug uptake as compared to tacrolimus solution alone. However, it was significantly less than tacrolimus solution containing verapamil with and without blank Nof-29 or tacrolimus loaded Nof-29 formulation clearly indicating that the blank DDS per se does not markedly affect the P-gp pump activity. The moderate increase in tacrolimus uptake can be attributed to the presence of numerous blank lipophilic oil cores that enhance the tacrolimus solubility in the aqueous environment. It could be deduced from the overall results of these experiments that the novel delivery system does not activate the P-gp since the pump does not recognize tacrolimus which is hidden in the coated oil cores of the nanocapsules.

Transport of Tacrolimus Across the Rat Intestinal Membrane

The permeation studies through the intestinal jejunum membrane should shed light on the combined role of P-gp efflux and Cytochrome P450 3A (CYP3A) as potential biochemical barriers to limit the passage of tacrolimus across the enterocytes (31) since Caco-2 cells do not express specifically CYP3A (33) that mainly metabolize tacrolimus (19–21). The results presented in Fig. 6, showing the passage from the apical to the basal side of the intestinal mucosa without serosa clearly support the results of the Caco-2 monolayer experiments. It can again be observed that both Prograf[®], the commercial product and the argan oil/oleoyl polyoxyglycerides emulsion did not enhance the permeation through the intestine (respective P_{app} values calculated from Eq. 3 of 209.3 ± 17.7 and $179 \pm 38.9 \times 10^{-6}$ cm/s) because of the

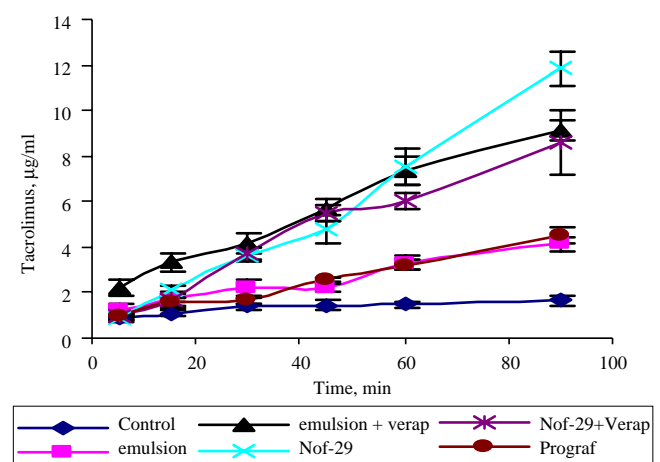


Fig. 6. Mucosal to serosal passage of tacrolimus across small intestine jejunum segment in various formulations. The concentration of verapamil when appropriate was 150 µg/ml. Data represents mean \pm SD, $N=4$.

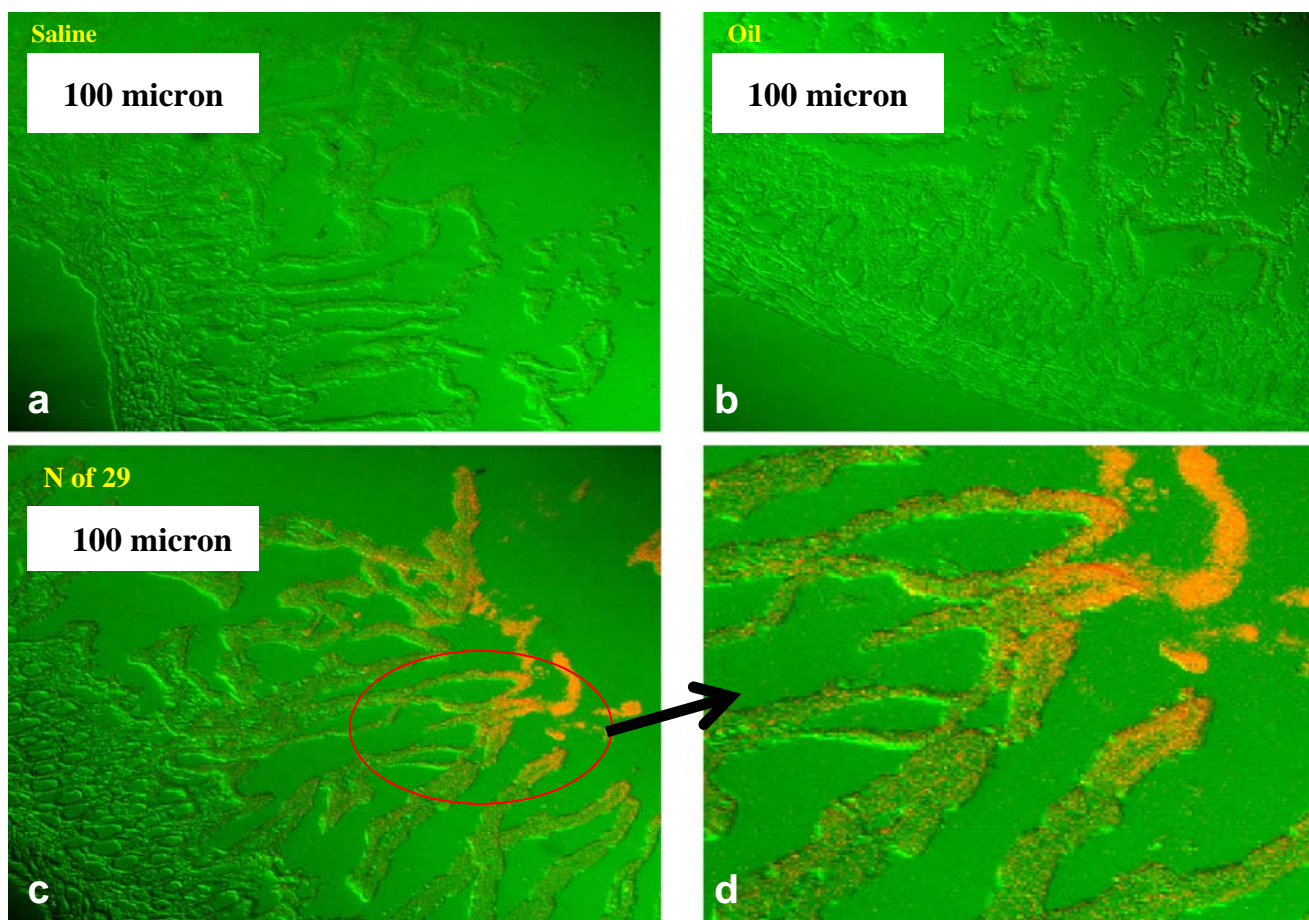


Fig. 7. Fluorescence photomicrographs of histological section of rat jejunum 30 min following oral gavage of **a** saline, **b** oil phase core and **c, d** microencapsulated nanocapsule formulation Nof-29 loaded with Nile red marker at 1 mg/ml oil phase. **c, d** Nile red nanocapsules at the jejunum lumen and adhering nanocapsules to the enterocyte membrane and in the cytoplasm of the enterocytes.

P-gp efflux and CYP450 enzymes. However, when tacrolimus reconstituted emulsion was combined with verapamil, tacrolimus permeation increased markedly as reflected by the P_{app} values of $480.8 \pm 76.8 \times 10^{-6}$ cm/s but still significantly less than the P_{app} value of $608.6 \pm 64.3 \times 10^{-6}$ cm/s yielded by Nof-29 (Fig. 6). The addition of verapamil to Nof-29 did not alter the absorption profile of tacrolimus (P_{app} value of $533.7 \pm 21.7 \times 10^{-6}$ cm/s) confirming that tacrolimus absorption was not influenced by the presence of the potent P-gp inhibitor and CYP3A substrate. These data confirm that the emulsion was not able to retain the tacrolimus within the oil droplets under the actual experimental conditions mimicking physiological conditions. Thus, tacrolimus was subjected to the metabolism effect of the CYP enzymes and efflux pump effect of P-gp resulting in a low passage of the drug to the serosal side of the intestine (Fig. 6). However, when the tacrolimus emulsion was combined with verapamil, tacrolimus permeation increased markedly but still significantly less than with Nof-29 (Fig. 6). The P_{app} values elicited by Nof-29 with and without verapamil did not differ. These data demonstrate and confirm again that the novel delivery system enhances the tacrolimus absorption by escaping the P-gp efflux pump effect and protecting the drug from the degradation effect of the CYP450 enzymes.

Histological Evaluation

The optical data depicted in Fig. 7a,b,c,d showed clearly the lack of any fluorescence in the enterocytes of the jejunum 30 min after the oral administration of Nile red loaded saline or oil core phase while Nof-29 formulation elicited the penetration of fluorescent lipophilic tiny droplets, presumably intact nanocapsules (Fig. 7c,d). These histological results indicated that the orally administered Nof-29 formulation was rapidly absorbed into the enterocytes lining the small intestine followed by the villar stromal cells engulfment. Due to the rapid absorption, it may be suggested that the administered nanocapsules penetrated un-hydrolyzed into the enterocytes. It can also be deduced from the data depicted in Fig. 7c,d that once the microspheres reached the jejunum, where the pH is above 7, they swelled and adhered to the mucosa owing to the presence of HPMC while the Eudragit L dissolved, creating large pores in the microsphere matrices. This allowed the diffusion of presumably intact Nile red loaded nanocapsules, although some molecular fluorescent marker diffusion cannot be excluded. Even though there is no evidence at this stage that intact nanocapsules internalized in the enterocytes, still numerous small lipophilic oil cores containing Nile red were detected in the enterocytes

and reached the lamina propria. Nevertheless, these results do support our hypothesis and further efforts should be made to elucidate clearly the absorption pathway of such nanocapsules and loaded active molecules from the novel delivery system. Animal experiments are being finalized and we will soon report on the potential of the novel DDS in enhancing the oral bioavailability of P-gp substrate drugs.

CONCLUSION

Preliminary encouraging *in vitro* and *ex vivo* results were achieved with an original delivery system consisting of lipid nanocapsules of tacrolimus embedded in a specific blend of Eudragit polymers together with HPMC. The highest drug uptake in the Caco-2 monolayer was achieved by the tacrolimus solution combined with verapamil, a well-known P-gp inhibitor and CYP3A substrate and the novel delivery system either alone or in combination with verapamil, suggesting that verapamil had no effect on tacrolimus absorption elicited by the delivery system. The blank formulation did not alter the P-gp pump activity. The results of the permeation studies through the intestinal jejunum membrane confirmed that the novel delivery system enhanced the tacrolimus absorption by escaping the P-gp efflux pump effect and protecting the drug from the degradation effect of the CYP450 enzymes. It was shown that once the microspheres reached the jejunum, they swelled and adhered to the mucosa due to the presence of HPMC while the Eudragit L dissolved creating large pores in the microsphere matrices allowing the diffusion of nanocapsules. The overall results suggest that the novel nanodelivery system is a potential platform for intestinal transport of sensitive lipophilic P-gp substrate molecules.

ACKNOWLEDGEMENT

This work was supported in part by a grant from the Chief Scientist Office of the Ministry of Trade and Industry (NOFAR program), Jerusalem, Israel and from Nanolymp Ltd., Rosh Ha'ayin, Israel. Simon Benita is affiliated with the David R. Bloom Center for Pharmacy at the Hebrew University of Jerusalem.

REFERENCES

1. B. Knight, M. Troutman, and D. R. Thakker. Deconvoluting the effects of P glycoprotein on intestinal CYP3A: a major challenge. *Curr. Opin. Pharmacol.* **6**:528–32 (2006).
2. L. Z. Benet, C. Y. Wu, M. F. Hebert, and V. J. Wachter. Intestinal drug metabolism and anti-transport processes: a potential paradigm shift in oral drug delivery. *J. Control. Release.* **39**:139–143 (1996).
3. V. J. Wachter, L. Salphati, and L. Z. Benet. Active secretion and enterocytic drug metabolism barriers to drug absorption. *Adv. Drug Del. Rev.* **20**:99–112 (1996).
4. M. Hennessy, and J. P. Spiers. A primer on the mechanics of P-glycoprotein the multidrug transporter. *Pharmacol. Res.* **55**:1–15 (2007).
5. T. Yamagata, H. Kusuhara, M. Morishita, K. Takayama, H. Benameur, and Y. Sugiyama. Improvement of the oral drug absorption of topotecan through the inhibition of intestinal xenobiotic efflux transporter, breast cancer resistance protein, by excipients. *Drug. Metab. Dispos.* **7**:1142–1148 (2007).
6. P. Breedveld, J. H. Beijnen, and J. H. Schellens. Use of P-glycoprotein and BCRP inhibitors to improve oral bioavailability and CNS penetration of anticancer drugs. *Trends Pharmacol. Sci.* **1**:17–24 (2006).
7. K. Y. Win, and S. Feng. Effects of particle size and surface coating on cellular uptake of polymeric nanoparticles for oral delivery of anticancer drugs. *Biomaterials.* **26**:2713–2722 (2005).
8. C. L. Cooper, R. P. van Heeswijk, K. Gallicano, and D. W. Cameron. A review of low dose ritonavir in protease inhibitor combination therapy. *Clin. Infect. Dis.* **12**:1585–92 (2003).
9. A. Owen, B. Chandler, and D. J. Back. The implications of P-glycoprotein in HIV: friend or foe? *Fundam Clin. Pharmacol.* **19**:283–96 (2005).
10. P. P. Constantinides, and K. M. Wasan. Lipid formulation strategies for enhancing intestinal transport and absorption of P-glycoprotein (P-gp) substrate drugs: *in vitro/in vivo* case studies. *J. Pharm. Sci.* **96**:235–48 (2007).
11. V. Risovic, M. Boyd, E. Choo, and K. M. Wasan. Effects of various lipid-based oral formulations on plasma and tissue amphotericin B concentrations and renal toxicity in male rats. *Antimicrob. Agents Chemother.* **47**:3339–3342 (2003).
12. B. J. Aungst. Novel formulation strategies for improving oral bioavailability of drugs with poor membrane permeation or presystemic metabolism. *J. Pharm. Sci.* **82**:979 - 986 (1993).
13. T. Gershanik, and S. Benita. Positively-charged self-emulsifying oil formulation for improving oral bioavailability of progesterone. *Pharm. Dev. Technol.* **1**:147 - 157 (1996).
14. D. T. O'Hagan, N. M. Christy, and S. S. Davis. Particulates and lymphatic drug delivery. In W. N. Chasmar, and V. J. Stella (eds.), *Lymphatic Transport of Drugs*, CRC, Boca Raton, FL, 1992, p. 279-315.
15. N. H. Shah, M. T. Carvajal, C. I. Patel, M. H. Infeld, and A. W. Malick. Self-emulsifying drug delivery systems (SEDDS) with polyglycolized glycerides for improving *in vitro* dissolution and oral absorption of lipophilic drugs. *Int. J. Pharm.* **106**:15 - 23 (1994).
16. D. J. Hauss, S. E. Fogal, J. V. Ficorilli, C. A. Price, T. Roy, A. A. Jayaraj, and J. J. Keirns. Lipid-based delivery systems for improving the bioavailability and lymphatic transport of a poorly water-soluble LTB₄ inhibitor. *J. Pharm. Sci.* **87**:164 - 169 (1998).
17. M. A. Fischl, D. D. Richman, C. Flexner, M. F. Para, R. Muebrich, A. Karim, P. Yeramian, J. Holden-Wiltse, and P. M. Meehan. Phase I/II study of the toxicity, pharmacokinetics, and activity of the HIV protease inhibitor SC-52151. *J. AIDS Hum. Retrovirol.* **15**:28 - 34 (1997).
18. A. Karim, R. Gokhale, M. Cole, J. Sherman, P. Yeramian, M. Bryant, and H. Franke. HIV protease inhibitor SC-52151: a novel method of optimizing bioavailability profile via a micro-emulsion drug delivery system. *Pharm. Res.* **11**:S368 (1994).
19. B. Kaplan, K. Lown, R. Craig, M. Abecassis, D. Kaufman, J. Leventhal, F. Stuart, H. U. Meier-Kriesche, and J. Fryer. Low bioavailability of cyclosporine microemulsion and tacrolimus in a small bowel transplant recipient. *Transplantation.* **67**:333–338 (1999).
20. K. Yokogawa, M. Takahashi, I. Tamai, H. Konishi, M. Nomura, S. Moritani, K. Miyamoto, and A. Tsuji. P-Glycoprotein-dependent disposition kinetics of tacrolimus: studies in *mdr1a* knockout mice. *Pharm. Res.* **16**:1213–1218 (1999).
21. H. Saitoh, Y. Saikachi, M. Kobayashi, M. Yamaguchi, M. Oda, Y. Yuhki, K. Achiwa, K. Tadano, Y. Takahashi, and B. J. Aungst. Limited interaction between tacrolimus and P-glycoprotein in the rat small intestine. *Eur. J. Pharm. Sci.* **28**:34–42 (2006).
22. C. U. Wu, and L. Z. Benet. Predicting drug disposition via application of BCS: transport/absorption/elimination interplay and development of a biopharmaceutics drug disposition classification system. *Pharm. Res.* **22**:11–23 (2005).
23. J. Schrickx, and J. Fink-Gremmels. P-glycoprotein-mediated transport of oxytetracycline in the Caco-2 cell model. *J. Vet. Pharmacol. Therap.* **30**:25–31 (2007).
24. Y. Gotoh, N. Kamada, and D. Momose. The advantages of the Ussing chamber in drug absorption studies. *J. Biomol. Screen.* **10**:517–523 (2005).
25. P. Anderle, E. Niederer, W. Rubas, C. Hilgendorf, H. Spahn-Langguth, H. Wunderli-Allenspach, H. P. Merkle, and P. Langguth. P-glycoprotein (P-gp) mediated efflux in Caco-2 cell

- monolayers: the influence of culturing conditions and drug exposure on P-gp expression levels. *J. Pharm. Sci.* **87**:(6) 757–762 (1998).
26. K. Manjunath, and V. Venkateswarlu. Pharmacokinetics, tissue distribution and bioavailability of clozapine solid lipid nanoparticles after intravenous and intraduodenal administration. *J. Control Release.* **107**:215–228 (2005).
 27. F. Foger, T. Schmitz, and A. Bernkop-Schnurch. *In vivo* evaluation of an oral delivery system for P-gp substrates based on thiolated chitosan. *Biomaterials.* **27**:4250–4255 (2006).
 28. H. Fessi, F. Puisieux, J. Devissaguet, N. Ammoury, and S. Benita. Nanocapsule formation by interfacial polymer deposition following solvent displacement. *Int. J. Pharm.* **55**:R1–R4 (1989).
 29. M. M. Crowley. Solutions, emulsions, suspensions and extracts. In: Remington: The Science and Practice of Pharmacy (21st edition), Lippincott Williams & Wilkins, Philadelphia, PA, 2005, pp 762
 30. V. C. Furtado Mosqueira, P. Legrand, H. Pinto-Alphandary, F. Puisieux, and G. Barratt. Poly (D,L-Lactide) Nanocapsules prepared by a solvent displacement process: Influence of the composition on physiochemical and structural properties. *J. Pharm. Sci.* **89**:614–626 (2000).
 31. A. M. Calcagno, J. A. Ludwig, J. M. Fostel, M. M. Gottesman, and S. S. V. Ambudkar. Comparison of drug transporter levels in normal colon, colon cancer and Caco-2 cells: impact on drug disposition and discovery. *Mol. Pharmacol.* **3**:87–93 (2006).
 32. T. Shimada, A. Terada, K. Yokogawa, H. Kaneko, M. Nomura, K. Kaji, S. Kaneko, K. Kobayashi, and K. Miyamoto. Lowered blood concentration of tacrolimus and its recovery with changes in expression of CYP3A and P-glycoprotein after high-dose steroid therapy. *Transplantation.* **74**:1419–1424 (2002).
 33. P. J. Trotter, and J. Storch. Fatty acid esterification during differentiation of the human intestinal cell line Caco-2. *J. Biol. Chem.* **268**:10017–10023 (1993).